PNAS
www.pnas.org

Supplementary Information for

DSCAM promotes self-avoidance in the developing mouse retina by masking the functions of cadherin superfamily members

Andrew M. Garrett, Andre Khalil, David O. Walton, Robert W. Burgess

Corresponding Author: Robert W. Burgess
Email: robert.burgess@jax.org

This PDF file includes:

Supplementary text
Figs. S1 to S6
References for SI reference citations

www.pnas.org/cgi/doi/10.1073/pnas.1809430115

Supplementary Methods

Fasciculation Score

In analogy with a mathematical metric space, each image considered here represents an element of that space and the output functions describe their various topological characteristics. The distance (metric) between each image in the metric space is obtained by considering the distance between their output functions, and then used to quantitatively classify the images in a complexity order. Those images that are closest to a uniform image (in this paper, an image where all pixels share a unique value) will have a low complexity score, while those that are farthest from this uniform image will have a higher complexity score. In this way, complexity quantifies "how far" an image is from uniformity. The *coordinate* of an image in this metric space is given by

$$\eta_g = d_E\left(g_\sigma, g_{\sigma_0}\right)$$

where g represents the output function, σ is the image under consideration, σ_0 is the uniform reference image, and d_E is the Euclidean-based metric:

$$d_E\left(g_\sigma, g_{\sigma_0}\right) = \int \left|g_\sigma(\Sigma) - g_{\sigma_0}(\Sigma)\right|^2 d\Sigma$$

where Σ is the threshold level value, from minimum to maximum pixel intensity.

The fasciculation score for each image was calculated by combining two output functions**.** The *distribution of density* (Figure S2A) characterizes the fraction m of the image at a pixel intensity value greater than a threshold value Σ:

$$m(\sigma;\Sigma) = \frac{\int \sigma(\mathbf{x})\Theta[\sigma(\mathbf{x}) - \Sigma]\mathrm{d}^2\mathbf{x}}{\int \sigma(\mathbf{x})\mathrm{d}^2\mathbf{x}},$$

where $\sigma(\mathbf{x})$ is the pixel intensity value of the image σ at position $\mathbf{x} = (x,y)$ and Θ is a step function. As the threshold value increases with the step function, m will decrease. In images showing fasciculation, dendrites fail to occupy the entire field, leaving black space. This is represented by a steeper slope of decrease in m over increasing threshold levels, illustrated in Figure S2A.

A set of connected pixels (allowing diagonal connections) is called a component. The histogram of the number of components as a function of the threshold value is an output function called the distribution of components, and is denoted $n(\sigma;\Sigma)$. The morphology of each component is quantified by the filament index

$$F = \frac{PD}{4A},$$

where P is the perimeter, D is the diameter (defined as the maximum length between any two points on the boundary of the component), and A is the area of the component. F=1 for a circle, and any value of $F > 1$ quantifies the departure of a component from a circular shape. The *distribution of filament indices* (Figure S2B) is

$$f(\sigma;\Sigma) = \frac{1}{n(\sigma;\Sigma)}\sum_j F_j,$$

where F_j is the filament index of the component j, with j going from 1 to $n(\sigma;\Sigma)$. This output function quantifies elongated image features. These features become more prominent in fasciculated images across all increasing threshold levels until the highest levels when components become disconnected (Figure S2B).

The *distribution of fasciculation, FASC,* (Figure S2C) is defined as the quotient of the filament indices over the density:

$$FASC(\sigma;\Sigma) = \frac{f(\sigma;\Sigma)}{m(\sigma;\Sigma)}.$$

Finally, for each image σ, the *fasciculation score (FS)* is the coordinate for the distribution of fasciculation

$$FS = \eta_{FASC} = d_E\left(FASC_\sigma, FASC_{\sigma_0}\right).$$

Since for a uniform reference image σ_0, both $f(\sigma_0;\Sigma)$ and $m(\sigma_0;\Sigma)$ yield constant values as a function of Σ, and therefore, so does $FASC_{\sigma_0}$, and since all images considered are compared to this same reference image, we can safely assume that $FASC_{\sigma_0}$ = 0. Thus, the fasciculation score is given by

$$FS = d_E(FASC_\sigma, 0) = \int |FASC_\sigma(\Sigma)|^2 \, d\Sigma.$$

The number of threshold values (Σ) used was 16. The minimum size for a set of connected pixels to be considered a component was 50 pixels. When no such components of this size were found at a given threshold, $f(\sigma;\Sigma)$ was set to 0. In theory, as the threshold level approaches the maximum pixel value, the distribution of density approaches 0 (i.e., as $\Sigma \to \infty$, $m(\sigma;\Sigma) \to 0$), which could cause concern since $m(\sigma;\Sigma)$ is the denominator in *FASC* (and we need to avoid dividing by zero). This was taken into account and divergence was avoided by only considering a finite number of threshold values (with the help of the step function Θ), by not considering the threshold value when Σ was equal to the maximal pixel value of the image, and by setting any value for $m(\sigma;\Sigma) < 10^{-6}$ equal to 10^{-6}. Also note that, empirically, setting a minimum component size at 50 pixels typically ensured that $f(\sigma;\Sigma)$ (and therefore $FASC(\sigma;\Sigma)$) was equal to zero at high threshold values (see Figure S2C).

To determine the level of significance when comparing the distributions of FS between each possible pair of genotypes, we ran a two-sided Wilcoxon rank sum test, which is appropriate for non-Gaussian distributions. The high variability and non-Gaussian nature of the FS distributions suggests that it might be incorrect to assume that the fasciculation phenotype will be homogeneously found in any given retina. Assuming instead that the fasciculation is heterogeneously distributed, it is possible that the imaging process randomly led to the collection of an image containing little or no fasciculation vs. another containing a significant amount. This "chance" can be quantified by dividing each image into four non-overlapping sub-images. Instead of just looking at the strength of the fasciculation (as quantified by the FS) within each sub-image, we can count the number of sub-images per genotype that have a FS above a certain threshold. Therefore, an additional statistical analysis of FS was performed.

From the *Dscam*$^{+/+}$ group, an objectively determined critical Fasciculation Score, FS_{crit}, was obtained by calculating the 95.45th percentile of the data. This is the equivalent of considering the mean + 2 standard deviations, but without having to worry about the Normal vs. non-Normal nature of the data. This corresponds to FS_{crit}=5,278. With this strategy, for any given image, if FS > FS_{crit}, then the image is considered to be fasciculated, and otherwise not. As expected, the proportion of *Dscam*$^{+/+}$ sub-images that are fasciculated is 4/88 (~4.5%). All other genotype sub-images were treated similarly. The 95% confidence intervals as well as the p-values for proportions when comparing *Dscam*$^{+/+}$ and *Dscam*$^{-/-}$ vs. all other genotypes were calculated according to (1).

Elo score

We developed a web-based system, called Image Echelon, to perform qualitative image comparisons using head-to-head matchups and an algorithm based on the Elo rating system for ranking chess players, as described previously (2, 3). At the beginning of each session, the user was presented with an example of a wild type "non-fasciculated" image and a mutant "fasciculated" image along with a brief description of the salient features to be compared. The user was then presented with two randomly selected images with the instruction to choose the image that looked more like the wild type. When the user chose an image, a new pair was immediately presented, allowing a user to quickly perform many comparisons. Each image started with a score of 1200, and an image's score was updated after each matchup according to the following Elo algorithm:

$$score_{new} = score_{old} + 10(outcome - expected)$$

The value for *outcome* is 1 for a win (i.e., the image chosen as more like wild type) and 0 for a loss (the image not chosen), while *expected* is a value between 0 and 1, determined by the difference in *score* between the two images entering the matchup. For a matchup between images A and B, *expected* for image A is described by the following formula:

$$expected_A = \frac{1}{1 + 10^{\frac{score_B - score_A}{200}}}$$

This results in an equal point exchange in each matchup where more points are exchanged in an upset than when the expected image wins. For historical reasons related to chess, all images started with a score of 1200. After completion, the scores were normalized to 0 (i.e., 1200 was subtracted from each final score).

This method was verified using the same image set as used for the Fasciculation Score. We had ten observers perform comparisons within the entire set of 150 images until 9696 matchups were completed, an average of 129 matchups per image. Scores from all images of three genotypes are plotted against matchup number in Figure S2D, demonstrating the consistent increase in *Dscam*$^{+/+}$ scores compared to the consistent decrease in *Dscam*$^{-/-}$ scores. Images from *Dscam*$^{-/-}$*:Cdh3*$^{-/-}$ acquired a score distribution intermediate between *Dscam*$^{+/+}$ and *Dscam*$^{-/-}$.

The endpoint of 9696 comparisons was chosen arbitrarily. To see how many matchups were required to separate the genotypes, we performed a pairwise Wilcoxon rank sum test at 10 time points from 800 total matchups to the endpoint. The statistic derived from each comparison was transformed into a standard score, or z-score, which describes by how many standard deviations the statistic deviates from the mean. The z-score for each comparison is plotted against matchup number in Figure S2E. Any pairwise comparison between *Dscam*$^{+/+}$*;other* and *Dscam*$^{-/-}$*;other* (where "other" is any other genotype, e.g., *Cdh3*, *Cdh6*, *Ctnna2*) surpassed the 95% confidence interval (i.e., z-score ±1.96) by about 2500 matchups and had stabilized by 3500 matchups. No pairwise comparisons between *Dscam*$^{+/+}$*;other* and *Dscam*$^{+/+}$*;other* reached significance or showed any indication that more matchups would cause them to do so. Pairwise comparisons between *Dscam*$^{-/-}$*;other* and *Dscam*$^{-/-}$*;other* include the intermediate phenotypes. Here again, z-scores are largely consistent from 3500 matchups until the endpoint. Thus, for this dataset, 3500 total matchups were sufficient to separate the genotypes, only 46 matchups per image and well below saturation of all possible comparisons.

To test how closely the fasciculation score correlated with the Elo score (Figure S2F), a power-law correlation analysis was performed, yielding a Pearson correlation coefficient of R=0.4198, which, for 150 samples represents a highly correlated pairing (p-value < 0.00001).

Supplementary Figures

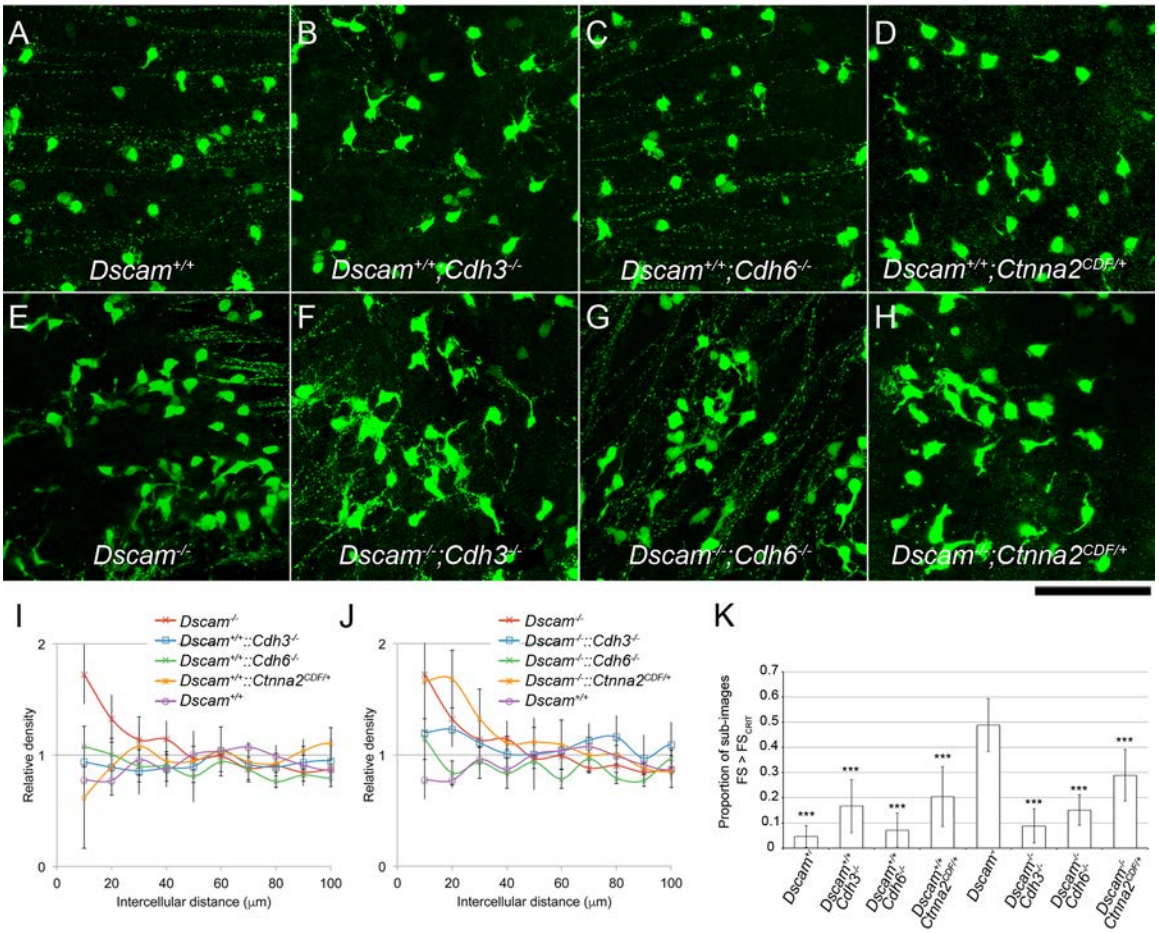

Figure S1: Loss of Cadherin-mediated adhesion does not reduce Cdh3-GFP-RGC cell body clustering. Cell body spacing for Cdh3-GFP-RGCs at P4 was analyzed in (**A**) wild type, (**B**) *Cdh3*$^{-/-}$, (**C**) *Cdh6*$^{-/-}$, and (**D**) *Ctnna2*$^{CDF/+}$ mutants alone, and (**E-H**) in combination with *Dscam*$^{-/-}$ mutants. **I**) The density recovery profile (DRP) plotted for each single-mutant shows no significant difference from control in the cadherin mutants. **J**) Likewise, when in combination with *Dscam*$^{-/-}$, the cadherin mutations did not significantly affect cell spacing. **K**) The FS scores represented in Figure 2 were compared to a threshold (FS_{crit}) defined as the value corresponding to the mean plus two standard deviations of wild type images. The proportions of images from each genotype with scores over FS_{crit} are presented. p-values of each genotype compared to *Dscam*$^{-/-}$ were calculated according to (1). n= 3-8 retinas per genotype (median = 6) over 1-4 microscope fields of view (median = 3 fields per retina). Scale bar 100 μm. *** is $p < 0.001$.

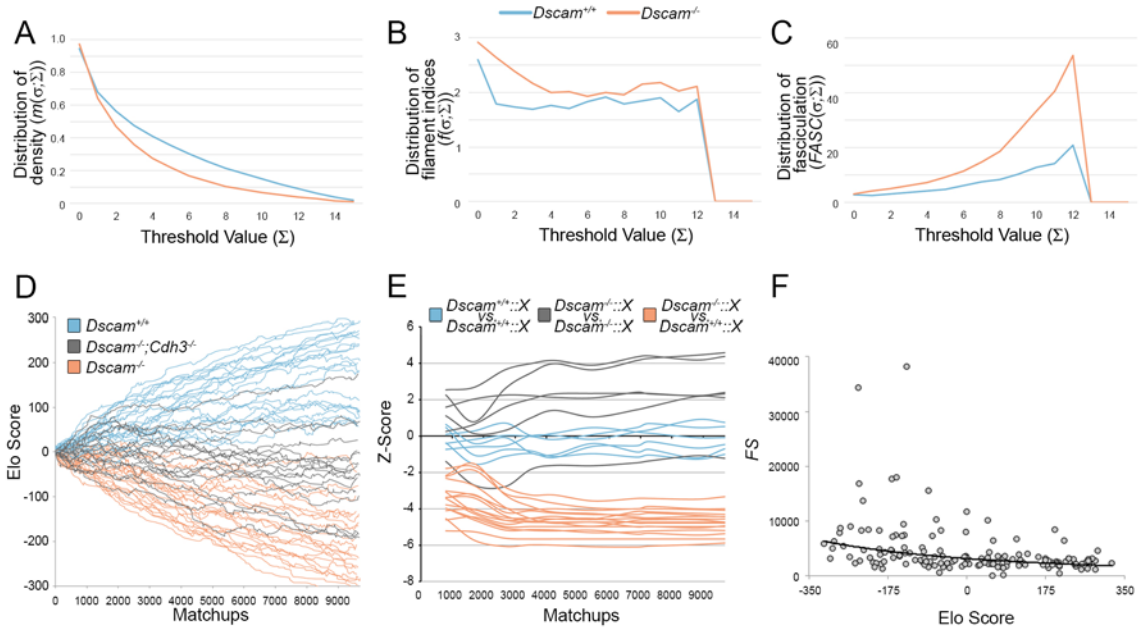

Figure S2: Methods to quantify spacing and fasciculation in Cdh3-GFP-RGCs. A-C) Example plots of the output functions used to calculate the FS score are presented for representative *Dscam*$^{+/+}$ and *Dscam*$^{-/-}$ images, including (**A**) the distribution of density ($m(\sigma;\Sigma)$), (**B**) the distribution of filament indices ($f(\sigma;\Sigma)$), and(**C**) the distribution of *FASC* ($FASC(\sigma;\Sigma)$). **D**) The Elo scores found using Image Echelon from all individual images of three genotypes – *Dscam*$^{+/+}$ (blue), *Dscam*$^{-/-}$ (orange), and *Dscam*$^{-/-}$*;Cdh3*$^{-/-}$ (gray) – are plotted against the total matchup number. *Dscam*$^{+/+}$ scores consistently increased, while *Dscam*$^{-/-}$ scores decreased. *Dscam*$^{-/-}$*;Cdh3*$^{-/-}$ images acquired intermediate scores. **E**) A pairwise Wilcoxon rank sum test was performed for all paired combinations of genotypes at 10 points between 800 and 9696 matchups. The resulting Z-scores are plotted against the total matchup number. All *Dscam*$^{+/+}$*:X* vs. *Dscam*$^{+/+}$*:X* comparisons are in blue, *Dscam*$^{-/-}$*:X* vs. *Dscam*$^{+/+}$*:X* comparisons are in orange, and *Dscam*$^{-/-}$*:X* vs. *Dscam*$^{-/-}$*:X* comparisons are in gray. Z-scores are largely stabilized by 3500 total matchups. **F**) Each full image is plotted according to its *FS* and Elo score. A power-law correlation analysis yielded a Pearson correlation coefficient of R=0.4198, which corresponds to $p < 0.00001$. n= 3-8 retinas per genotype (median = 6) over 1-4 microscope fields of view (median = 3 fields per retina). Scale bar 100 μm.

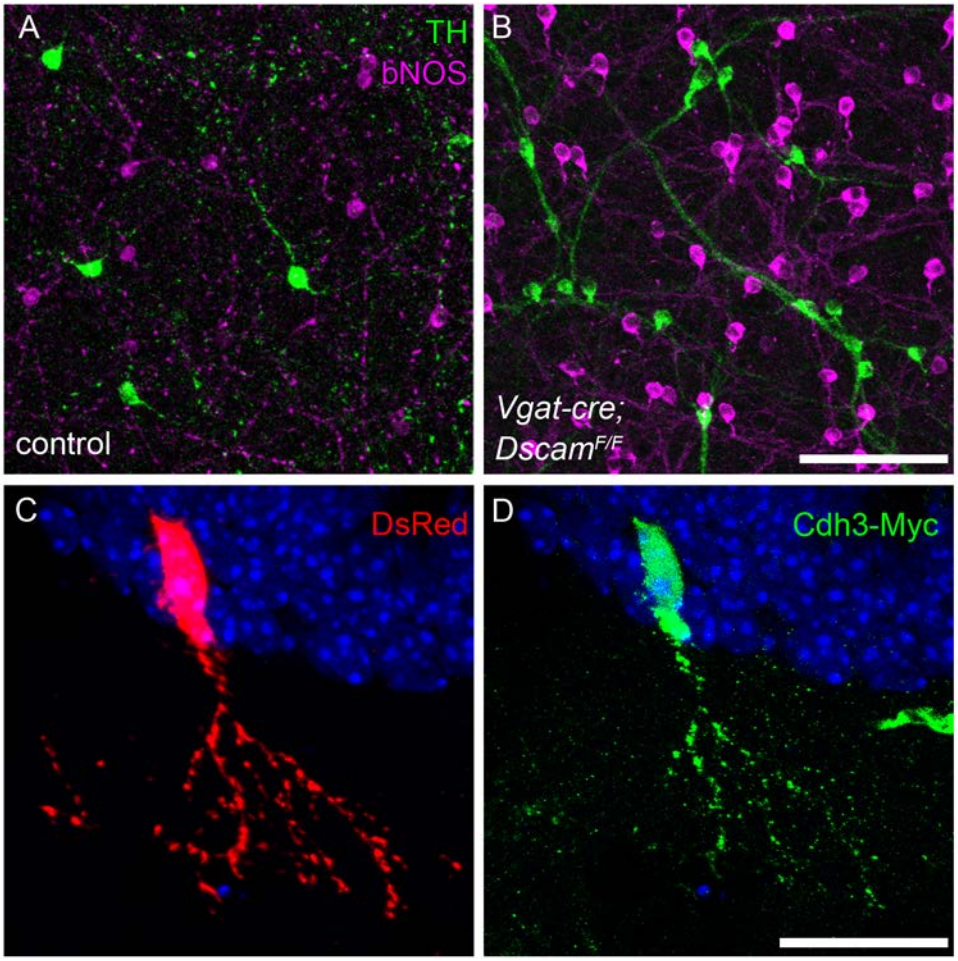

Figure S3: Co-electroporation in Vgat-Cre retinas. A) Retinas from control (**B**) and *Vgat-Cre:Dscam*$^{F/F}$ mice were stained for TH+ amacrine cells (green) and bNOS+ amacrine cells (magenta). Both amacrine cell types formed clusters and fascicles in the conditionally mutant retinas. **C-D**) When pCALNL-DsRed and pCALNL-Cdh3 were co-electroporated into Vgat-Cre retinas, co-expression was observed in cells morphologically consistent with amacrine cells. Scale bar is 100 μm in **A**,**B** and 20 μm in **C**,**D**.

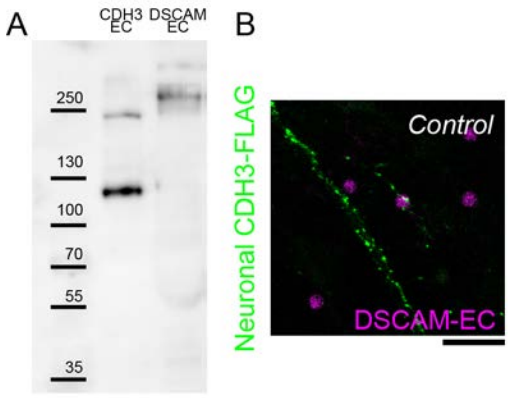

Figure S4: Recombinant ectodomains. A) FC-tagged recombinant CDH3 and DSCAM ectodomains isolated from media are the expected size by Western blot. Note the CDH3 sample also retains a minor band consistent with dimerization. **B**) When beads coated with DSCAM-EC alone were applied to neurons transfected with Cdh3-FLAG, beads had no effect on CDH3 clustering.

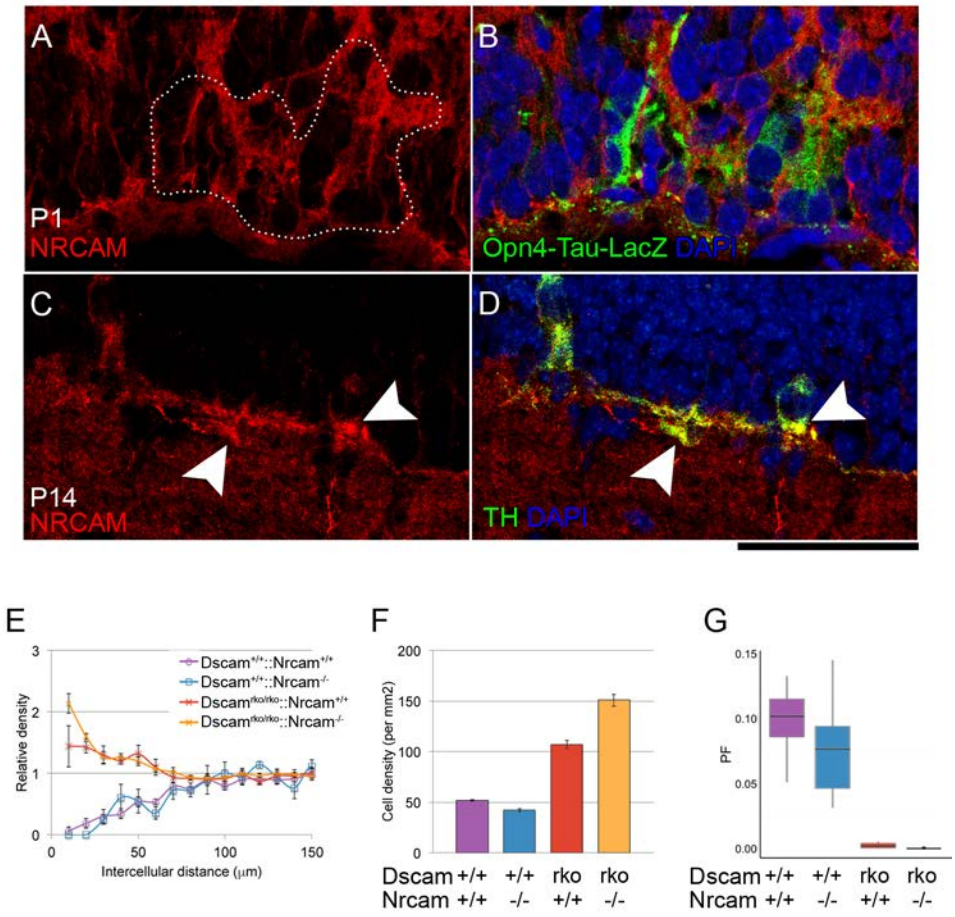

Figure S5: NRCAM is enriched in DA cells and ipRGCs. Cryosections from *Dscam*$^{-/-}$ retinas were immunostained for NRCAM (red). **A-B**) At P1, NRCAM was enriched in ipRGC cell clusters, labeled for βGal in Opn4-Tau-LacZ animals (green). **C-D**) At P14, NRCAM was visible at DA cell neurite fascicles (arrows) labeled for tyrosine hydroxylase (green). **E-G**) *Nrcam* mutation did not significantly affect DA cell body spacing or number. n= 6 retinas per genotype over 2-4 microscope fields of view (median = 3 fields per retina). Box plots represent the median, first and third quartile, range, and outliers. Scale bar is 50 μm in **A-D** and 100 μm in **E-J**.

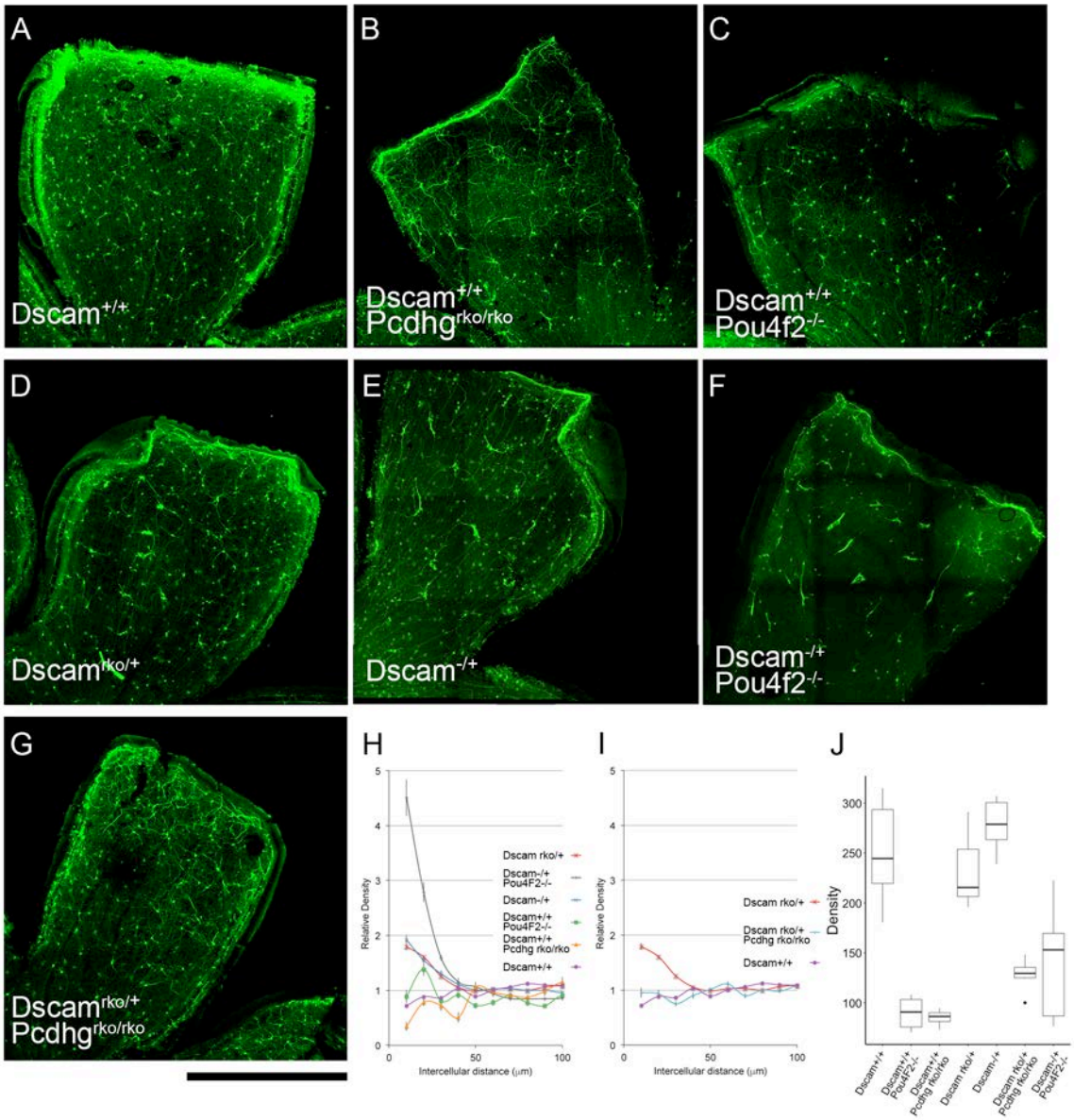

Figure S6: γ-Pcdh-mediated adhesion contributes to ipRGC clustering. A-G) Representative images of whole retina quadrants illustrate the types of images used to quantify ipRGC spacing and fasciculation in Figure 6. **H-J**) Cell body spacing of ipRGCs was analyzed from images of 0.6 mm^2 microscope fields near the periphery of the retina. Clustering was identified in *Dscam* heterozygous mice by DRP. Reducing cell number in Pou4f2 mutation did not rescue this spacing

defect, but loss of γ-Pcdh-mediated adhesion did. n= 6 retinas per genotype over 2 microscope fields of view per retina.

References

1. Freund JE (1992) *Mathematical Statistics* (Prentice Hall College Division) 5 Ed.
2. Elo AE (1978) *The rating of chessplayers : past and present* (Arco Publishing, New York) p 208 p.
3. Garrett AM, Tadenev ALD, Hammond YT, Fuerst PG, & Burgess RW (2016) Replacing the PDZ-interacting C-termini of DSCAM and DSCAML1 with epitope tags causes different phenotypic severity in different cell populations. *eLife* 5:e16144.